Aerodynamically Generated Acoustic Resonance (AGAR) Model Revisited and Refurbished

M. Grossi[*†], M. Laureti[*] and B. Favini[*]
[*]*Dept. of Mechanical and Aerospace Engineering - Sapienza University of Rome*
Via Eudossiana 18, 00184 - Rome, Italy
marco.grossi@uniroma1.it · mariasole.laureti@uniroma1.it · bernardo.favini@uniroma1.it
[†]Corresponding author

Abstract

The aim of this paper is to investigate the vortex-sound modeling and its impacts on AGAR model prediction capabilities, considering as test case a POD-Y-like SRM. The mathematical model has been revisited and enriched in order to take into account two-phase effects. This activity represents, thus, a further step in the consolidation and validation of the AGAR model for the characterization of pressure oscillations in aft-finocyl SRMs which is fundamental for both the in operation launch vehicle, i.e. VEGA, and the future ones, i.e. Ariane 6 and VEGA-C/VEGA-E.

1. Introduction

A number of large segmented solid rocket motors, including Ariane 5 P230[2,10], US Space Shuttle boosters[26] and the Titan family[4,9], are reported to exhibit pressure oscillations (PO) during operation. Also monolithic aft-finocyl motors, e.g. VEGA first stage P80[21] and mid-scale demonstrator POD-Y SRM,[16,17] are prone to develop the same problematic. Although they do not compromise the motor life, such oscillations may represent an important issue, which has to be accounted for at the system level. Their occurrence has to be carefully evaluated in order to correctly assess the pressure oscillations time windows and amplitude which represents an input for the structures dimensioning, above all, for the stage interfaces, equipment and the payload adapter, in order to correctly characterize the dynamic environment. In fact, pressure oscillations of the order of about 0.5 % of the mean value, due to the transfer function between pressure and thrust, can generate thrust oscillations about 5 % of the mean thrust value. Since the bulky employ of Solid Rocket Motors (SRMs) in the current and future European space transportation system, these issues are nowadays of crucial importance and are worth of deep investigation.

At the present state-of-the-art, the chief mechanisms of instabilities in solid rockets could come from both propellant combustion and hydrodynamic flow field instabilities.[8] For large segmented motors, however, active research during the past years showed that instabilities are generally dominated by a coupling between chamber acoustics (mostly axial modes) and hydrodynamic instability. The latter arises from vortex shedding stemming either from unstable shear layers (caused by an obstacle, such as a protruding inhibitor,[31,32] or by specific grain shapes[14]), or surface instability.[22] This phenomenon has been supported via both experimental[1] and numerical[22] approaches, and has occurred to be a powerful source of instability in large segmented solid rockets. The same may be affirmed also for monolithic aft-finocyl motors, anyway, in these last the scenario is decidedly more challenging since it is impossible to make a such clear distinction between vortex sources because of the grain morphology that may give rise to complex vorticity patterns, which, moreover, are strongly affected by the grain composition itself. This one consists of a multi-component mixture of oxidizer particles and metallic additives (especially aluminum) bound together by a combustible polymeric binder. Plasticizers, stabilizers and burn rate modifiers can be also present causing an overall heterogeneity in mass and energy flow rate of the combustion products injected in the chamber.

Along with hydrodynamic instabilities and combustion inhomogeneity, multi-phase effects play an important role in PO development. Aluminum droplets released in the chamber are ignited and constitute an additional energetic contribution to thrust the rocket. The gaseous products released from the burning droplets condense to form an aluminum oxide cap and finally yield inert droplets which behave as a source of acoustic losses for pressure oscillations.[8,33] Besides such dumping effect, aluminum combustion may be able to drive and amplify instabilities.[3,28] Indeed if characteristic time scales of distributed combustion and chamber acoustics coincide, a possible thermo-acoustic limit cycle could appear. Such phenomenon is named ITHAC (Instabilitié s THermo-ACoustique).[12,13,18,27]

This work is devoted to the investigation of the results obtained by numerical simulations of PO phenomenon in aft-finocyl SRMs built my means of the AGAR (Aerodynamically Generated Acoustic Resonance) model, a Q1D single-phase model already developed and validated, in which pressure oscillations are recovered thanks to the coupling between hydrodynamic instabilities and acoustics modes[11, 29, 30] . In recent past AGAR has demonstrated to possess prediction and reconstruction capabilities in a wide range of aft-finocyl SRMs. Indeed pressure oscillations trends have been captured on both POD-Y and P80 motors,[20, 29] in particular for this last a complete reconstruction of PO dispersion has been provided.[21] On the other hand it is worth highlighting that for Zefiro 23 SRM and Zefiro 9 SRM, respectively second and third stage of VEGA launch vehicle, not prone at all to PO phenomena by experimental evidence, the AGAR model does not show any aeroacoustic coupling, demonstrating that when a motor is not prone to pressure oscillations, the model does not provide them.

The purpose of this paper lays in the discussion of PO numerical solution modification provided by some new features recently introduced in the model concerning vorticity source and two-phase effects. Since the lack of a true multi-phase description, the model itself does not distinguish the different contributions leading to the onset of pressure oscillations. For such reason in AGAR model vorticity has to be regarded as a "generalized vorticity" (called POX), which includes turbulence as well as distributed combustion of solid phase. In order to explicit the consequence of having solid particles both burning and inert in the flow field, the employ of proper and tailored source terms in the Euler set of equations has thus been taken into account. In next sections the effect of such elements will be first mathematically depicted and then numerically tested on the POD-Y-LIKE SRM. Such motor represents a mock-up version of POD-Y SRM, reconstructed by the authors on the basis of open literature data, by means of an in-house code devoted to the generation of a 3D propellant grain surface.[6, 20]
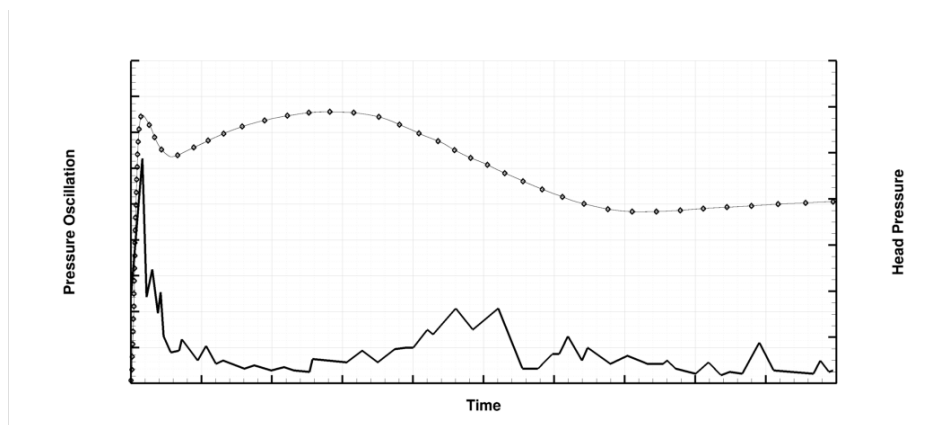
(a) POD-Y experimental pressure oscillations and head pressure[16, 17] .
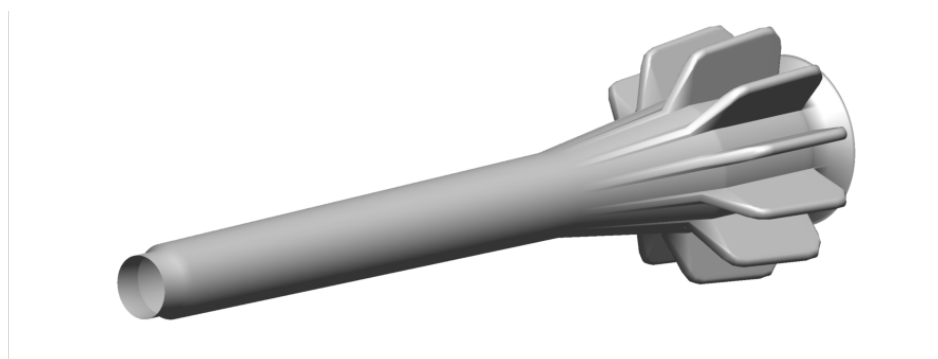
(b) POD-Y-LIKE geometry evaluated on open literature.

Figure 1: POD-Y-LIKE pressure curves and geometry.

2. AGAR Aeroacoustics Mathematical Model

The model developed for the pressure oscillations simulation during the SRM internal ballistics, named AGAR, is composed by the following two modules: a grain burnback simulation tool (GREG - Grain REGression, based on a level set technique properly tailored to the evolution of the combustion surface of the SRMs) and a flow field solver

for the internal ballistics, based on a single-phase unsteady Q1D Eulerian formulation of the SRM flow field, enhanced to account for aeroacoustic phenomena. In order to provide an enrichment of AGAR modeling and to improve the physical content of its already developed characteristics, a general review of some crucial properties of the model has been performed. In this section such new features are analyzed and fully investigated in the frame of AGAR aeroacoustics model.

In a Q1D fashion, vorticity is naturally neglected in the Euler set for single-phase flow, however describing its dynamics is possible thanks to a further equation. The reduced vorticity equation is formally derived from the multi-dimensional one introducing the assumptions of axisymmetric flow and added to the complete Euler set. Anyway due to the physical phenomenology and aft-finocyl geometry, some simplification can be exploited to describe vortex dynamics. In aft-finocyl configuration vorticity generated along the forward cylinder is carried towards the motor nozzle exit and released into the flow-field as a result Corner Vortex Shedding (CVS) occurring where the geometry is sharp enough to allow the stream separation. In AGAR model, such vorticity is not directly reproduced, but arises thanks to proper source terms (see Eq.4) from the separation point located where CVS takes place. Usually such point is addressed to be at the entrance of the star region and will be, for sake of simplicity, called step. A generation criterion based upon pressure evolution evaluated at the step controls vortices releasing timing and thus vortex-shedding frequency.

The complete mathematical set of equations solved in AGAR model follows:

$$\frac{\partial \left(\rho A_p \right)}{\partial t} + \frac{\partial \left(\rho u A_p \right)}{\partial x} = s_{prop}^{(m)} + s_{cav}^{(m)} \tag{1}$$

$$\frac{\partial \left(\rho u A_p \right)}{\partial t} + \frac{\partial \left[\left(\rho u^2 + p \right) A_p \right]}{\partial x} - p \frac{\partial A_p}{\partial x} = s_{POX}^{(q)} \tag{2}$$

$$\frac{\partial \left(\rho e A_p \right)}{\partial t} + \frac{\partial \left[\left(\rho e + p \right) u A_p \right]}{\partial x} = s_{prop}^{(e)} + s_{cav}^{(e)} + s_{POX}^{(e)} \tag{3}$$

$$\frac{\partial \left(\omega A_p \right)}{\partial t} + \frac{\partial \left(k_u u \omega A_p \right)}{\partial x} = s_\omega + s_{p-g} \tag{4}$$

Source terms s_{prop} and s_{cav} in mass and energy equations, are originated from, respectively, propellant combustion and cavity modeling to take into account the submergence zone located close to the motor nozzle. For a thorough depiction of AGAR concerning such characterization, complete descriptions are available in previous works.[5,19]

Focusing on Eq.4, two modeling contributes are added to the standard Q1D equation for vorticity dynamics: s_ω and k_u. The first represents the instantaneous vorticity source enabled on the shedding point, whereas the second one is a correction coefficient introduced to take into account that, because of the Q1D formulation itself, the vorticity advection velocity is different from the one evaluated thanks to a Q1D model. Finally s_{p-g} term, introduced in AGAR model by means of this paper, takes into account the aerodynamic gas-particle coupling acting on vorticity dynamics.

In accordance with the Lighthill-Powell-Howe vortex-sound theory,[15,25] acoustic emissions are provided by the misalignment between acoustic and vortices velocity vectors. In AGAR such excitement is introduced thanks to proper source terms in momentum and energy balance laws. They derive directly from the manipulation of the Euler equations employing the Laplace identity to explicit the vorticity contribute. Their expressions are the following:

$$s_{POX}^q = \rho u \frac{dR_p}{dx} A_p \omega \tag{5}$$

$$s_{POX}^e = u \, s_{POX}^q \tag{6}$$

2.1 Vorticity Transport Discussion

For what concerns the k_u parameter, it is, as in recent papers[20,29] constrained to the following functional law:

$$k_u(t) = \alpha_u \frac{u_{step}(t)}{u_{step}(0)} \tag{7}$$

where α_u is a simple proportionality constant whose value is changed in order to do parameter inquiring, taking care, however, to keep it always very close to unity. To relate the k_u parameter to SRM flow field, we can observe that, due to its trend, it represents the balance at the step between the cylindrical and the finocyl region mass injections.

In particular, the flow velocity at the step follows the evolution of the burning surfaces of the cylindrical and of the aft-finocyl regions.

The k_u parameter affects the lock-in condition, thus PO time windows of occurrence and, more indirectly, PO amplitude, since its relation with the vortex-shedding frequency which will be clearly seen in next sections.

A hint of the effect of modulating the k_u parameter around the functional law of Eq.7 has been already studied and analyzed in a very recent paper concerning P80 PO dispersion.[21] In this work exploiting a free k_u has allowed to modify the coupling condition, assuring a plain recover of pressure oscillations envelopes in spite of the full lack of two-phase modeling. Anyway if k_u is tied to respect a well defined function, only the enrichment of the mathematical model with some two-phase features permits to deal with PO characterization. This topic is actually investigated in the next section.

2.2 Vorticity Source Discussion

The vorticity source term s_ω is currently modeled through a functional law which states that, in presence of vortex-shedding phenomena, the vorticity piled up during the time lapse between two consequent vortex releasing, T_ω, is related to the square of the step free stream velocity[7,23,24]. Anyway, looking at the nature of the problem itself, an enhanced characterization is introduced in order to account for the generalized vorticity production level within the SRM combustion chamber ahead of the shedding location. Such concept results to:

$$s_\omega(t) = \alpha_\Gamma \, S_{b,cyl} \, u^2_{step} \, G(t, T_\omega) \tag{8}$$

where $S_{b,cyl}$ means the cylinder burning surface and α_Γ, since its role played in Eq.8, is represented by the inverse of a surface and can be thought as a direct measure of propellant composition effect on vorticity production. The last term, $G(t, T_\omega)$, is a dimensionless function employed to define the shape of s_ω in time. The signal currently chosen is a saw-tooth one whose slope and lasting are controlled by G in the following manner:

$$G(t, T_\omega) = \frac{t}{T_\omega} \tag{9}$$

The choice of modeling s_ω structure by means of the aforesaid formulation aims to properly depict the vorticity fluxes acting within the motor. Indeed vortices arise from the burning surface upstream the vortex-shedding point (typically at the end of the cylinder zone) and deeply depends on the propellant nature. It is important to point out that, with such formulation, beyond pure vorticity production α_Γ accounts also for the effect of aluminum droplets distributed combustion, a key feature of tho-phase flow. On the other hand, aerodynamic forces, are involved in the s_{p-g} source term.

2.3 New Two-phase Source Term

Notwithstanding AGAR is based upon a single-phase formulation, the effect of not-gaseous inert particles provided by the aluminum combustion may be introduced in the vorticity equation thanks to a tailored contribute.
Such source terms may be obtained by the employ of aerodynamic drag forces acting on the fluid by particles. This last may be written as:

$$\vec{F}_{p-g} = \frac{1}{2}\rho_g \, \pi R^2 \, C_D \, N_p \, |\vec{u}_p - \vec{u}_g| \, (\vec{u}_p - \vec{u}_g) \tag{10}$$

where R is the particle radius and N_p the number of solid particles per unit of volume. Anyway, since the lack of a proper two-phase model, particles properties can not be directly evaluated as well as their velocity, therefore the drag force truly employed in AGAR is approximated thanks to a calibration parameter, named χ, which is an estimation of aerodynamic properties and velocity relative difference. Taking into account Eq.10 in the momentum conservative form and the hereafter considerations, the vorticity equation handling already exploited in Eq.4 yields an enriched formulation of the vorticity dynamics in which s_{p-g} is the outcome of applying the curl operator on the aerodynamic force and averaging on the port area:

$$s_{p-g}(t) = \chi(t) \, u \, \omega \, A_p \tag{11}$$

It is worth noting that in order to maintain a rigorous view in which the particles can only have a drag role and thus are continuously sped up by fluid motion, χ is a negative quantity (having assumed $u, \omega \geq 0$).

Including a two-phase feature in AGAR model leads to a certain modification in the meaning of the vorticity source calibration parameter α_Γ. Making directly explicit some of the two-phase phenomenology allows to reduce

the physics hidden in α_Γ since, now, aerodynamic drag feature is accounted for by its own contribute. Actually, notwithstanding both phenomena (aerodynamic forces and distributed combustion) have the same origin (two-phase flow), in AGAR model they are split between two different source terms with their own calibrations.

3. Numerical Results

The aforementioned model has been applied and tested on the POD-Y-like SRM working on four different meshes whose properties are reported in Tab.1.

For what concerns the vorticity generation source, the α_Γ used for these simulations arises directly from the one employed in P80 set-up,[21] taking in mind the peculiar POD-Y propellant formulation. The latter, namely Butalane® Zen, has been designed to reduce aluminum distributed combustion role in PO amplification. In AGAR model, as previously mentioned, α_Γ accounts for both vortex strength and combustion instability, thus, its value is decidedly lower in the POD-Y-LIKE SRM with regard to the one exploited in P80 set-up. On the other hand, once vorticity source calibration is specified for one mesh, since numerical issues arising from different dissipation level occurring when grids are subject to refinement, the other meshes have to employ distinct α_Γ which, however, are chosen in order to match the first blow amplitude. It is important underling that this operation do not compromise the solutions: if the lock-in condition between acoustics mode and vortex-shedding does not subsist, PO will not show up no matter α_Γ values are chosen.

Table 1: Mesh properties.

Mesh	Coarse	Medium	Fine	Very Fine
Number of points (head-throat)	200	400	800	1600
Cell dimension h (m^{-2})	1.09	0.545	0.2725	0.1362
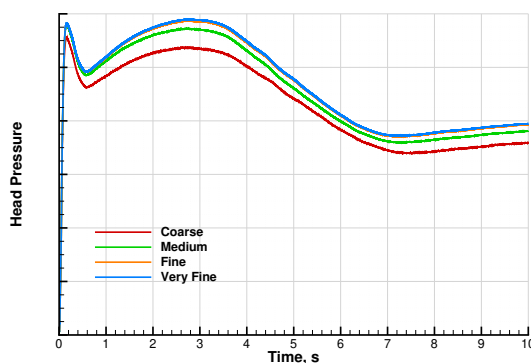
Figure 2: POD-Y-like head pressure evaluation employing different discretization.

A comparison of mesh resolution on head pressure is presented in Fig.2. Increasing the points number, pressure rises up mainly due to a modification of geometry properties (in particular the burning surface) thanks to a better capturing of grain profiles executed by GREG pre-processing operation. Anyway, focusing on the fine meshes it is clear enough that the numerical solutions are very close, witnessing the grid convergence.

3.1 Pressure Oscillations response at $\chi = 0$

The unsteady behavior of the head pressure evaluated by means of AGAR model not considering particles acting, i.e. $\chi(t) = 0$, is reported in Fig.3 for all the grids.

Looking at these figures some comments can be made. From a general point of view, the amplitude are lightly higher than the experimental curve, which is true especially for the coarse mesh. This last and the medium grid show up a PO plateau lasting up to the ending of the second blow, whereas the finer meshes present a more fluctuating envelope. Anyway, in all four solutions the overall PO level is in good agreement with measured data, a fact which confirmed how α_Γ has been well modeled. Moreover a plain recovery of the two major blows can be observed: the strong peak soon after ignition and the following lower structure occurring between $4 - 6\,s$. It is worth to note that simulations
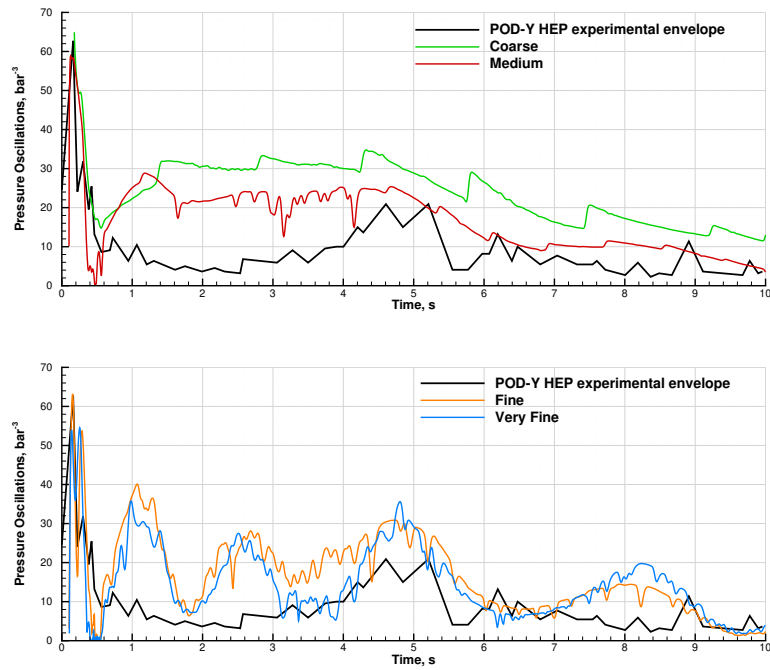
Figure 3: POD-Y-like pressure oscillations solution evaluated without aerodynamic forces contribute.
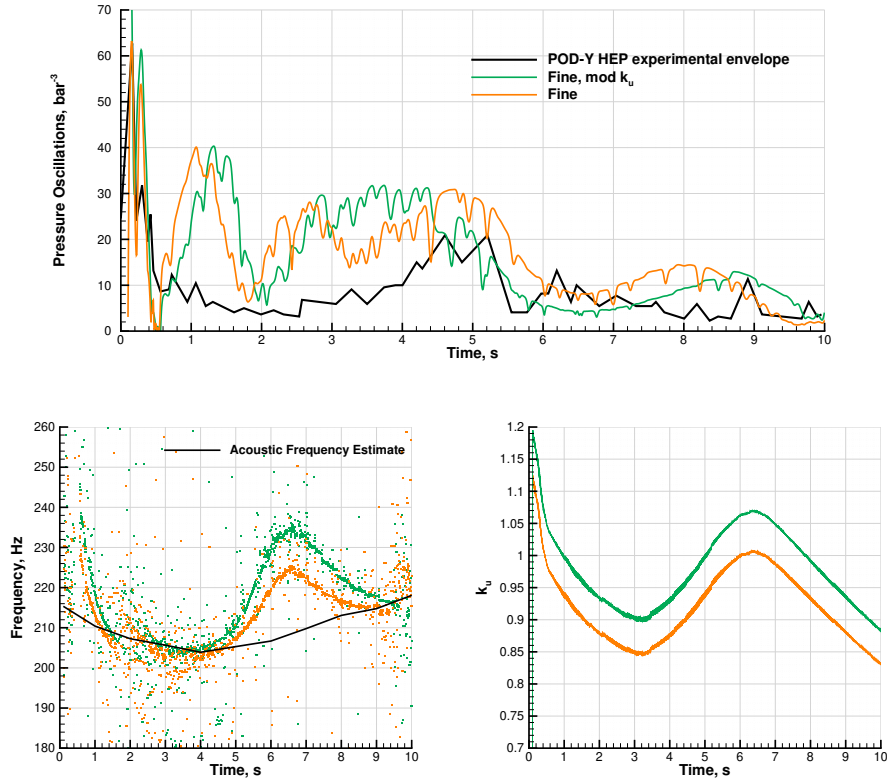
Figure 4: Pressure oscillations, vortex-shedding frequency and k_u parameter evaluated on the fine grid for two different values of α_u.

carried on the same POD-Y mock-up version proposed in previous papers[29, 30] do not show up any similarity between experimental data and numerical solutions regarding the first blow, a fact which testifies the goodness of the general review performed on AGAR model.

In order to investigate the effect of k_u on pressure oscillations time windows, a solution built on the fine mesh with a α_u value greater than the one employed in the previous simulations, is reported and compared in Fig.4. Note that k_u is always close to unity, indicating that the correction with reference to the Q1D velocity is by the way quite mild.

The strong relation between k_u and vortex-shedding frequency is clearly visible, since the higher the k_u, the greater the shedding frequency. Such dependency entitles, consequently, this calibration function to the direct control on the aeroacoustics coupling which relates vorticity dynamics timing and chamber acoustics. This last is the only source of pressure oscillations in AGAR model as it can be easily seen in the Fig.4, where PO rise up only when vortex-shedding frequency crosses or at least get closer to the acoustic motor one, providing well confined PO time windows.

3.2 Pressure Oscillations response at $\chi \neq 0$

Results just considered have been evaluated without applying any drag forces acting on the flow. If such two-phase feature is enabled in the model, pressure oscillations response undergo some modifications visible in Fig.5. Concerning the $\chi(t)$ time trends chosen to run such simulations, they are reported in Fig.6.
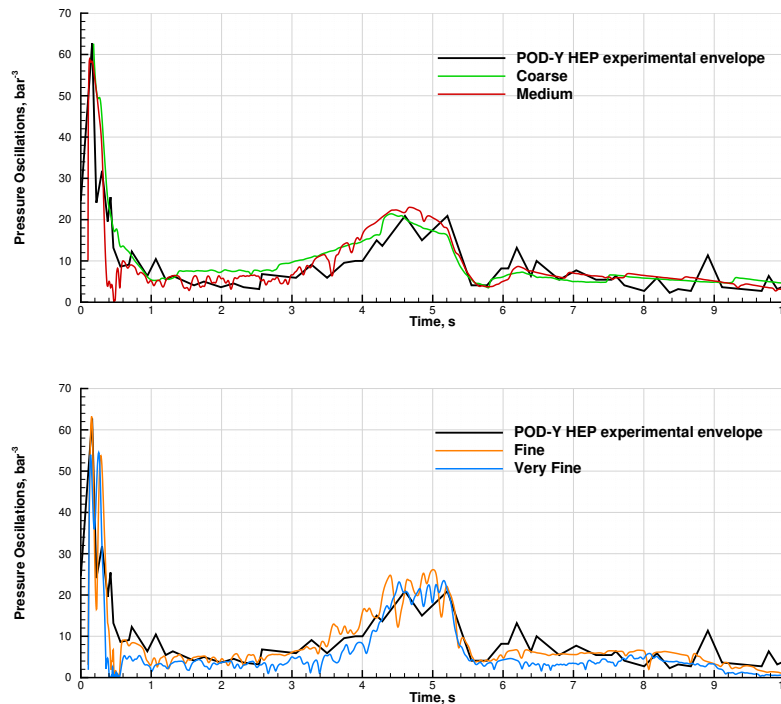
Figure 5: POD-Y-like pressure oscillations solution evaluated with aerodynamic forces contribute.

Including two-phase effect in vorticity dynamics described in Eq.4, whose action is modulated by χ parameter according to Fig.6, leads to an improvement of the agreement between numerical and experimental data. Indeed exploiting the presence in the flow field of particles slower than the gas phase, i.e. $\chi \leq 0$, provides a dumping effect on pressure oscillations envelopes which allows AGAR solutions to reduce the gap with measured data. Note, moreover, that leaving aside the coarse mesh, all other grids use the same χ function, suggesting that its effect is little affected by grid resolution.

Such statement can not be applied also to the connection between k_u and χ. Indeed in order to recover the same PO envelope, a modification of one of the two parameter will inevitably result in the other adjustment. This is justifiable considering the role played by these two contributes. If k_u is such to provide a lock-in condition, vorticity source level, fixed on the basis of propellant mixture composition, is able to establish PO envelope global amplitude. Two-phase effects acting as aerodynamic forces work modulating instantaneously vortices dissipation and transport, acting, thus, on pressure oscillations level and time windows. As a consequence, when k_u, hence vortex transport
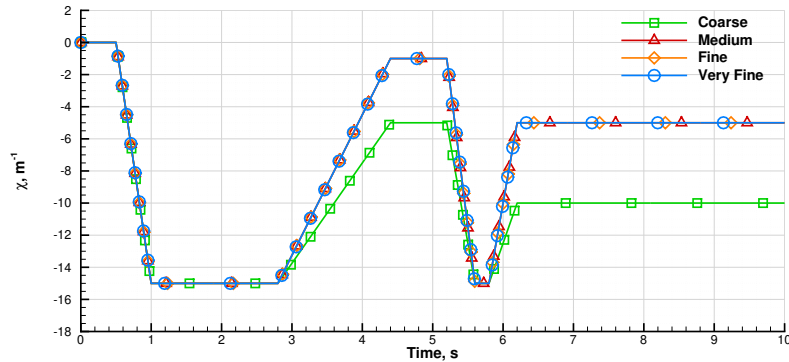
Figure 6: Calibration parameter χ time trend for all employed meshes.
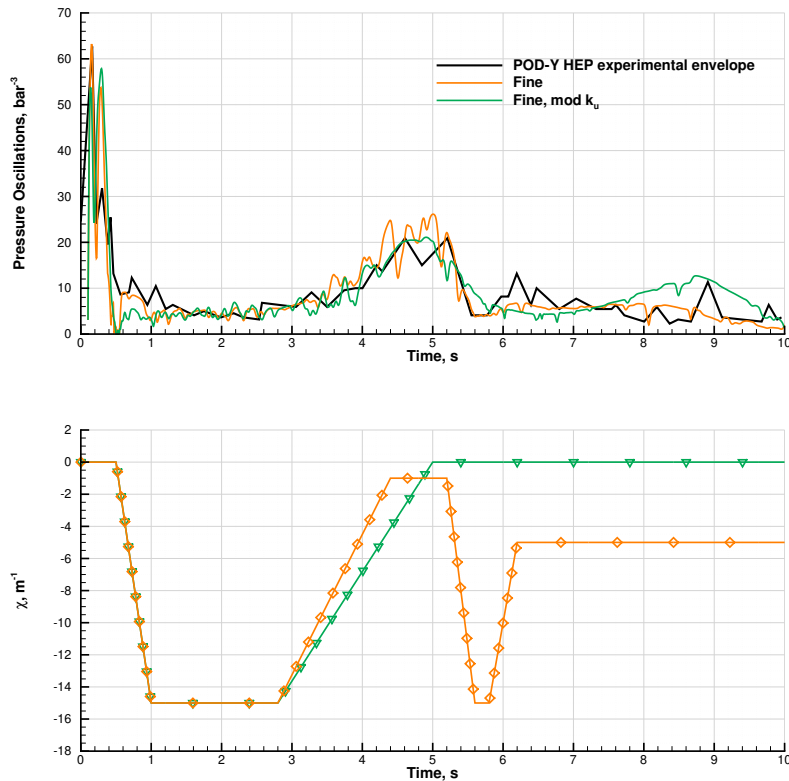
Figure 7: Pressure oscillations and χ parameter evaluated on the fine grid for two different values of α_u.

properties, is modified, pressure oscillations change shape and amplitude due to different lock-in conditions, therefore the same specific PO solution may be obtained only working on gas-particles forces.

4. Conclusions

The AGAR model provides the numerical simulation of pressure oscillations in aft-finocyl SRMs with a Q1D model employing a single-phase flow description, based on the assumption that PO show up due to the presence of a coupling between vortex-shedding phenomena and acoustic modes. Two closure terms are used to properly characterize hydrodynamic instabilities involved in the motor: k_u is the correction coefficient for the vorticity flow advection with respect to the Q1D average velocity, which affects mainly the pressure oscillation time windows and another, s_ω, is the vorticity generation term that models the amount of vorticity generated upstream the aft-finocyl region, mainly

affecting the pressure oscillation amplitude.

In this work, this last feature has been formulated through a functional law involving the cylinder-like region surface and a constant coefficient to take into account propellant mixture tendency to provide distributed combustion instabilities. Since the nature of the POD-Y propellant, it has been chosen a value considerably lower than the one exploited for conventional mixtures.

In order to account for multi-phase effects, a tailored source term has been proposed and applied to the Q1D vorticity equation. This term is directly modeled on the basis of the aerodynamic forces acting between the gaseous and solid phase. Since the lack of a rigorous two-phase model this new source needs a calibration term which takes into account aerodynamic properties.

The new version of AGAR, enriched with the aforementioned characteristics, have been tested on a mock-up version of the POD-Y SRM through the employ of four grids. The numerical results have shown that the proposed s_ω and k_u functional laws allow, without enabling two-phase effects, to obtain for all meshes a thorough good level of agreement between pressure oscillations measured data and numerical solutions. The PO response to aerodynamic forces has been further investigated. The employ of dissipative contribute, i.e. particles slower than gas, has provided an improvement of the numerical solutions, witnessing the dumping effect on pressure oscillations provided by solid particles.

This activity represents a further step towards the investigations of the AGAR model capability in the simulation of the pressure oscillation phenomena of aft-finocyl SRMs. In particular it demonstrates how an enrichment in the physical model allows a better recover of experimental data. Anyway in this context some challenges are inevitable. Since the Q1D formulation a full description of the plain physical phenomenon from which pressure oscillations arise requires a great modeling effort and the inescapable presence of calibration which, in turn, needs a large amount of dedicated experimental data that, currently, are missing especially in case of aft-finocyl SRMs.

References

[1] G. Avalon, G. Casalis, and J. Griffond. Flow instabilities and acoustic resonance of channels with wall injection. July 1998. AIAA Paper 98-3220.

[2] S. Ballereau, F. Godfroy, J.F. Guery, and D. Ribereau. Assessment on analysis and prediction method applied on thrust oscillations of Ariane 5 solid rocket motor. Huntsville, AL, July 2003. 39th AIAA Propulsion and Energy Forum and Exposition. AIAA Paper 2003-4675.

[3] K.P. Brooks and M.W. Beckstead. Dynamics of aluminum combustion. *Journal of Propulsion and Power*, 11(4):769–780, 1993.

[4] R.S Brown, R. Dunlap, S.W. Young, and R.C. Waugh. Vortex shedding as a source of acoustic energy in segmented solid rockets. *Journal of Spacecrafts and Rockets*, 18(4):312–319, 1981.

[5] E. Cavallini, B. Favini, and A. Neri. Q1D Modelling of Vortex-Driven Pressure Oscillations in Aft-Finocyl SRMs with Submerged Nozzle Cavity, 2015. Orlando, Florida.

[6] E. Cavallini, B. Favini, and A. Neri. Motor scale and propellant geometry effects on pressure oscillations in aft-finocyl solid rocket motors, 2016. Salt Lake City, Utah.

[7] R.R. Clements. An inviscid model of two-dimensional vortex shedding. *Journal of Fluid Mechanics*, 57(2):321–336, 1973.

[8] F.E.C. Culick. Unsteady motions in combustion chambers for propulsion systems, 2006. RTO AGARD RTO-AG-AVT-039.

[9] K.W. Dotson, S. Koshigoe, and K.K Pace. Vortex shedding in a large solid rocket motor without inhibitors at the segment interfaces. *Journal of Propulsion and Power*, 13(2):197–206, 1997.

[10] Y. Fabignon, J. Dupays, G. Avalon, F. Vuillot, N. Lupoglazoff, G. Casalis, and M. Prévost. Instabilities and pressure oscillations in solid rocket motors. *Aerospace science and technology*, 7(3):191–200, 2003.

[11] V. Ferretti. Numerical simulations of acoustic resonance of solid rocket motor, 2011. Ph.D. thesis.

[12] S. Gallier and F. Godfroy. Aluminum combustion driven instabilities in solid rocket motors. *Journal of Propulsion and Power*, 25(2):509–521, 2009.

[13] J.F. Guéry, S. Ballerau, F. Godfroy, S. Gallier, O. Orlandi, P. Della Pieta, E. Robert, and N. Cesco. Thrust oscillations in solid rocket motors. Hartford, CT, July 2008. AIAA Propulsion and Energy Forum and Exposition.

[14] J.F. Guéry, S. Gallier, P. Della Pieta, and F. Godfroy. Numerical simulations of thrust oscillations of segmented AP/AL solid rocket motors. October 2001. IAF 01-S.2.05.

[15] M.S. Howe. *Acoustics of Fluid-Structure Interactions*. 1998. New York: Cambridge Univ. Press.

[16] S. Larrieu. Demonstration of pressure oscillation reduction for a new large monolithic motor. Rome, Italy, May 2016. Space Propulsion. Paper n. 3125096.

[17] S. Larrieu, F. Godfroy, O. Orlandi, E. Robert, A. Ciucci, and N. Cesco. Demonstration of Pressure Oscillation Reduction in the Frame of New Launchers Development. Krakov, Poland, July 2015. 6th European Conference for AeroSpace Sciences.

[18] S. Larrieu, O. Orlandi, F. Godfroy, and C. Di Trapani. Two minutes inside P120C SRM. Seville, Spain, 2018. Space Propulsion 2018.

[19] M. Laureti and B. Favini. Pressure oscillations in aft-finocys SRMs. San Diego, California, 2019. AIAA SciTech Forum.

[20] M. Laureti, B. Favini, and G. Rossi. Aeroacoustics of Aft-Finocyl Solid Rocket Motors. Cincinnati, Ohio, 2018. AIAA Propulsion and Energy Forum and Exposition.

[21] M. Laureti, B. Favini, and G. Rossi. P80 SRM pressure oscillations reconstruction. Cincinnati, Ohio, July 2018. AIAA Propulsion and Energy Forum and Exposition.

[22] N. Lupoglazoff and F. Vuillot. Parietal vortex shedding as a cause of instability for long solid propellant motors. numerical simulations and comparisons with firing tests. January 1996. AIAA Paper 96-0761.

[23] K.I. Matveev. Reduced-order modeling of vortex-driven excitation of acoustic modes. *Acoustics Research Letters Online*, 6:14, 2005.

[24] K.I. Matveev and F.E.C Culick. A model for combustion instability involving vortex shedding. *Combustion Science and Technology*, pages 1059–1083, 2003.

[25] S.C. Morris. Shear-layer instabilities: Particle image velocimetry measurements and implications for acoustics. *Annual Review of Fluid Mechanics*, 43, 2011.

[26] T. Nesman. RSRM chamber pressure oscillations: Full scale ground and flight test summary and air flow test results. AIAA Propulsion and Energy Forum and Exposition, July 1995.

[27] O. Orlandi, M. Plaud, F. Godfroy, S. Larrieu, and N. Cesco. Aluminium droplets combustion and SRM instabilities. EUCASS, 7th European Conference for AeroSpace Sciences, 2017.

[28] R.L. Raun and M.W. Beckstead. A numerical model for temperature gradient and particle effects on Rijke burner oscillations. *Combustion and flame*, 94(1):1–24, 1993.

[29] G. Rossi, M. Laureti, B. Favini, E. Cavallini, and A. Neri. Aerodynamic Sound Levels in Aft-Finocyl Solid Rocket Motors. Atlanta, Georgia, 2017. AIAA Propulsion and Energy Forum and Exposition.

[30] G. Rossi, M. Laureti, B. Favini, E. Cavallini, and A. Neri. Vortex-Sound Modelling in Aft-Finocyl Solid Rocket Motors. EUCASS, 7th European Conference for AeroSpace Sciences, 2017.

[31] P.H. Shu, R.H. Sforzini, and W.A. Foster. Vortex shedding from solid rocket propellant inhibitors. June 1986. AIAA Paper 86-1418.

[32] A.K. Stubos, C. Benocci, E. Pallo, G.K. Stoubos, and D. Olivari. Aerodynamically generated acoustic resonance in a pipe with annular flow restrictors. *Journal of Fluids and Structures*, 13(6):755–778, 1999.

[33] S. Temkin and R.A. Dobbins. Attenuation and dispersion of sound by particulate-relaxation processes. *The Journal of the Acoustical Society of America*, 40(2):317–324, 1966.